Technical Article

The Divertor Tokamak Test facility, a challenge in the road map toward fusion energy: electromagnetic aspects of the project

***Abstract* — The energy problem is one of the main challenges of this century. It is a problem of *quantity*. New needs continue to come from emerging countries to support their industrial developments and population growth as well as to improve their living standards. Specific studies predict a doubling of demand over a few decades. It is also a question of *quality*. The sensitivity to the environment and to the future of the planet imposes a critical revision on the use of some of the present sources of energy and urges to search for new ones.**

Controlled thermonuclear fusion (CTF), based on the use of the same process occurring in the sun, is a very promising candidate to provide an important share in the basket of energy supply of a medium-term future. Strengths are the extremely wide availability of the fuel, the very limited environmental impact and the high safety standards. Electromagnetism plays a dominant role in magnetically confined fusion devices.

In the context of the European road map towards the commercial use of CTF, the Divertor Tokamak Test facility (DTT) project was approved, aimed at studying some critical aspects of the future commercial reactor, with an important investment (about 500 M€ and 1000 ppy for construction, more than 3000 ppy for operations).

What is fusion? When will a commercial fusion plant be in operation? What is the DTT mission? What about the electromagnetic heart of DTT? This note tries to answer these questions, providing the community of numerical electromagnetism with some information about its role and discussing some relevant aspects of this challenging program.

I. FUSION: WHAT AND WHY?

Fusion [1] is the nuclear reaction that, combining isotopes of light elements, produces elements of greater atomic number. The reaction is strongly exogenous because it produces elements with reduced mass nucleons and, as a consequence, the disappearance of mass - according to the Einstein equation - yields an enormous energy production.

Controlled thermonuclear fusion (CTF) is a promising way to produce alternative energy. The most adequate reaction for the first generation of commercial reactors (Fig. 1) combines two isotopes of hydrogen (Deuterium and Tritium) to produce Helium, a neutron and, moreover, an energy of 17.6 MeV.

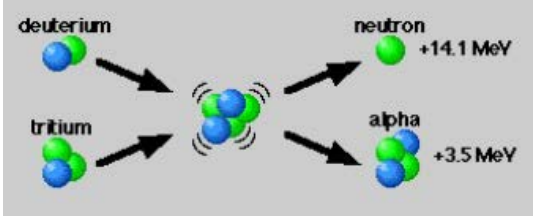

Fig. 1. D-T Fusion Reaction (courtesy of ENEA).

The fusion can take place only if the colliding atoms are so energized to be able to overcome electromagnetic repulsive forces and, as a consequence, to fall back into the sphere of influence of nuclear forces. In thermonuclear fusion, only plasmas at temperatures in the order of hundred million degrees can produce fusion reactions.

Fusion should not be invented, since it already exists in nature. The sun is a fusion reactor (Fig. 2). Its energy generates and feeds life on earth. Its energy has also generated the traditional fuels - coal, oil and gas - that we still use for our needs. They, indeed, come from the fossilization of organic matter to which, in the past millions of years, the sun had allowed life.

Fig. 2. Fusion Activity in SUN (courtesy of NASA).

The mechanism of energy generation in the sun, hypothesized by Eddington in 1920 was fully confirmed in 1938 by Bethe (Nobel Prize in 1967). After the first realization for military uses (1950 H-Bomb), the international community found a broad agreement on cooperation for the peaceful use of the fusion.

The CTF is very attractive for several important reasons.

- Limited environmental impact. No impact on the greenhouse effect as CO_2-free. Unlike fission reactors, currently operational, CTF does not produce any radioactive waste. The activation times within the plant can be limited to a few tens of years if a suitable choice of materials is made.
- High safety standards. The actual amount of fuel in the reactor is so limited as to exclude any risk of chain reactions: a technical accident (such as breaking the containment system or losing of the plant control) or a natural catastrophe (such as an earthquake and a devastating flood) or, finally, military aggression, would be naturally solved in the rapid interruption of the fusion reactions and in the extinction of the process of generation.
- Wide availability of fuel. Fuels (deuterium and lithium) are so widespread in nature that their availability appears to be superior to any reasonable need, in a realistic historical perspective.

However, the encouraging prospect of a practically inexhaustible fuel will be balanced by the need for extremely sophisticated technologies and, at least initially, very high

investment costs. Experts in economics, geography and sociology will be able to examine the impacts that the CTF will have on the redistribution of wealth on earth.

Long and complex is the path of research aimed to carry out the commercial use of the CTF. In the last half century, the size of experiments is moving from a few centimeters to several meters requiring efforts of thousands of man-years and billions of euros. With these so impressive needs, the individual effort of a single nation is certainly useless. Therefore, a first powerful and incontrovertible result has been already reached: a strong and deep scientific cooperation able to overcome frontiers, cultures, races and political orientations. For example, ITER [2], the main project presently in progress sees a strong cooperation between USA and Russia, China and India, the European Union and the Japan, to mention the main ones.

To allow to reach the fusion temperatures, the gas must be "confined", i.e. detached from every physical wall. The confinement can be classified in two main categories: "inertial", carried out by means of a fast heating operated by lasers, or "magnetic" which uses the capacity of the magnetic fields to generate pressures in ionized gases and, therefore, to act as real case. In the following, we will refer to the magnetically confined fusion.

The heart of the CTF is electromagnetism. The main subsystems of a fusion reactor are all based on electromagnetic fields: from the ionization of the gas to the plasma heating, from the control of the shape and position to the prevention of instability, from the confinement to the management of energy transformation. The main reason lies in the fact that, at the temperatures of interest, the fuel is necessarily in the form of a completely ionized gas.

Various configurations have been proposed. Interesting are the stellarators [3] like Wendelstein 7-X, presently operating in Greifswald, Germany, and the reversed field pinch [4] like the Reversed Field Experiment, RFX, operative in Padua, Italy. However, the most promising configuration is the Tokamak [5], proposed in the 1950s. It is a closed system, with a quasi-axis-symmetric toroidal shape, that entrusts the creation, heating and confinement of the plasma to appropriate magnetic fields of spatial and temporal form. In Fig. 3 a schematic view of a Tokamak is reported.

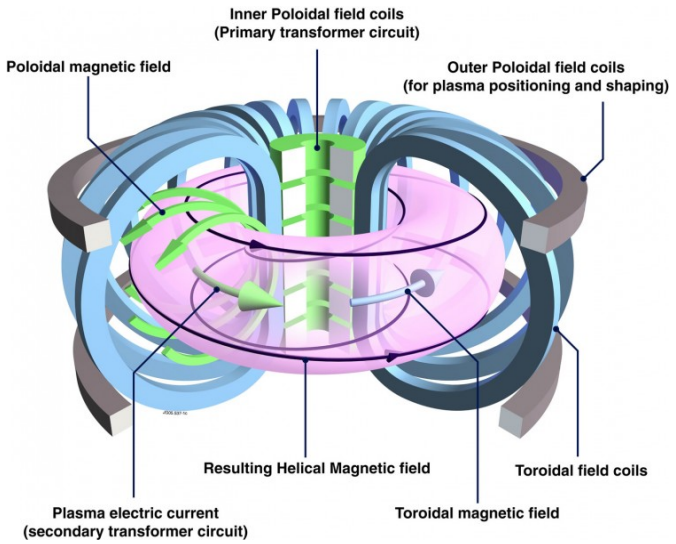

Fig. 3. Schematic view of the Tokamak (courtesy of EUROfusion).

The list of its main Tokamak subsystems includes:

- the magnetic system for the generation of both a toroidal field, for the confinement and stability of the plasma, and of a poloidal, for the control of its shape and equilibrium. The magnetic system includes also transformer coils for the induction of the electromotive forces necessary to induce a current in the plasma. Thanks to the current, the plasma -for ohmic effect- is heated and -for the interaction with the poloidal fields- is kept in balance and controlled. In order to limit the losses and to increase the magnetic field, most of the devices currently in operation and all those in planning use superconductor coils;
- a mechanical structure, including a vessel with adequate holding capacity of the high vacuum and, in addition, a cryostat to contain the cold area of the machine. An appropriate remote handling system ensures safe machine maintenance even during its operating life;
- an additional heating system based on antennas (for coupling with plasma electrons -Electron Cyclotron Radiofrequency Heating, ECRH- or ions -Ion Cyclotron Radiofrequency Heating, ICRH) and on high energy Neutral Beam Injection, NBI, to increase the plasma temperature;
- a sophisticated diagnostic system for accurate plasma monitoring and a control system for the shape and position of the plasma and for the counteracting of instabilities.

Therefore, the perspective CTF looks very promising. But when will it able to provide commercial electricity?

II. Fusion electricity: when?

National and international programs in CTF have been investing huge resources for several decades with a significant number of engineers and scientists. In the 90's the JET tokamak achieved one of the main missions of the European fusion program, producing 16 MW of nuclear fusion power from D-T reactions, at the price, however, of about 25 MW of input heating power needed to keep the machine in operation, i.e., with a fusion gain between nuclear power and losses $Q>0.6$.

To improve the fusion gain, the current research strategy aims to increase magnetic field, plasma current and machine dimensions. This is the mission of the already mentioned ITER experiment [2], an international tokamak under construction at Cadarache, France (Fig. 4). The idea of this international joint experiment was launched in 1985 and the first plasma is expected in 2025. In the next decades ITER should produce 500 MW of fusion power from 50 MW of input heating power with a fusion gain $Q\approx10$.

Fig. 4. Panorama of the ITER site during construction in March 2018. Credit © ITER Organization, http://www.iter.org/.

ITER will prepare the way for first electricity commercial production to the grid by fusion. In this respect the various ITER Members have their own plans. In 2012 European Fusion Development Agreement (EFDA) published a document on the

European Fusion Roadmap, revised in 2018 [6] by EUROfusion, a consortium that supports and funds fusion research activities on behalf of Euratom. The European Fusion Roadmap proposes a strategic vision toward the generation of electrical power by a Demonstration Fusion Power Plant (DEMO) to be completed in the second half of this century.

III. The DTT device: ID Card

A. Role and objectives

The European Fusion Roadmap [6] elaborated 8 strategic missions to tackle the main challenges in achieving the ambitious goal of first electricity commercial production to the grid by controlled nuclear fusion. In particular, mission n. 2 ("Heat-exhaust system") is aimed at carrying out alternative solutions to the problem of disposing the heat load.

The confinement in a tokamak is the result of magnetic field lines forming a set of closed, nested magnetic surfaces. At the edge of the plasma (Fig. 5), a thin (order of few millimeters) region with open field lines appears (Scrape-Off Layer, SOL). In a steady state magnetically confined fusion plasma, the power produced by fusion reactions needs to be extracted from the device. Charged particles (and their related energy), flowing out from the core plasma through the SOL, are directed to the plates of a narrow region of the chamber, called divertor [7], towards the separatrix (the last closed magnetic surface).
The heat flux parallel to the magnetic field, in the SOL region of ITER and DEMO, is expected to be comparable to that on the sun's surface.

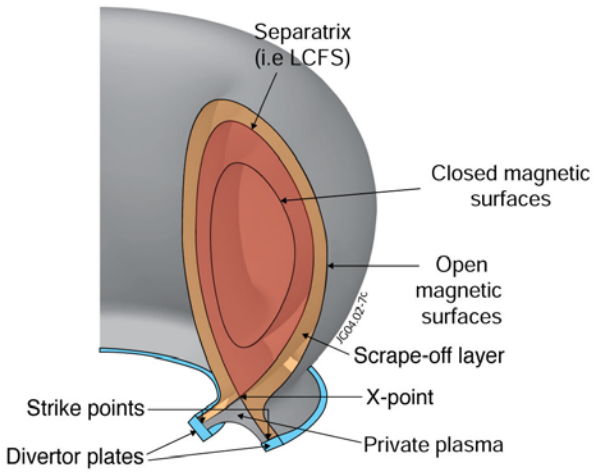

Fig. 5. Plasma edge: geometry of Scrape-Off Layer (SOL) and divertor plate (courtesy of EFDA-JET).

In ITER it is planned to test the capabilities of a baseline divertor operating in a plasma fully detached condition, i.e. without contact between plasma and solid walls. This can be obtained with high recycling conditions to high density and strong impurity radiation loss. In this way the SOL temperature drops below the ionization threshold, the particles become neutral and are not any more constrained by the magnetic field. Consequently, no direct energy flow is channeled to the divertor plates. This solution could be unsuitable to be extrapolated to the operating conditions of DEMO and future commercial reactors. Thus, the problem of thermal loads on the divertor may remain unresolved in the road to the realization of the reactor. For this reason, within the European Fusion Roadmap, a specific project has been launched, aimed to define and design a "Divertor Tokamak Test" facility (DTT). The mission of DTT is to carry out a number of scaled experiments, to be integrated with the specific physical condition expected in DEMO, with technological solutions applicable to future fusion plants. DTT is a facility: it is designed to test different divertor magnetic configurations, with solid and liquid metal divertor targets, and other possible solutions promising to face with the power exhaust problem.

DTT (Figs. 6-7) is a tokamak designed in Italy by ENEA (Agenzia nazionale per le nuove tecnologie, l'energia e lo sviluppo economico sostenibile), CREATE (Consorzio di Ricerca per l'Energia, l'Automazione e le Tecnologie dell'Elettromagnetismo), RFX (Consorzio RFX), CNR (Consiglio Nazionale delle Ricerche), with the contribution of several universities [8-9]. However, it is part of the general European programme in fusion research, which includes many other R&D actions like experiments, modeling tools, and technological developments for liquid divertors. The specific role of the DTT facility is to bridge the gap between today's proof-of-principle experiments and the DEMO reactor, in the specific field of the energy exhaust treatment. DTT should have the specific mission to bring such solutions to a sufficient level of maturity and integration from both physics and technology points of view.

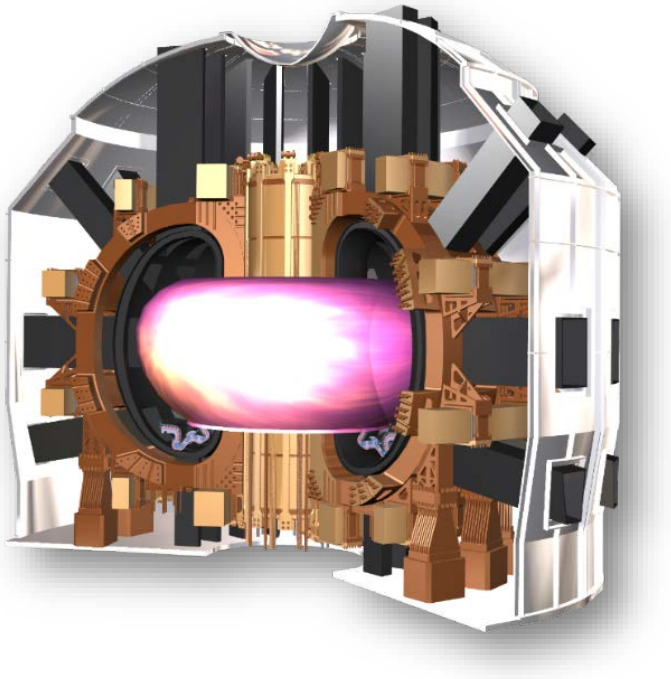

Fig. 6. DTT artistic view.

Fig. 7. Rendering image of the DTT conceptual layout in an advanced phase of the assembly in Frascati, Italy.

The investment costs of about 500 M€ will be bore mainly by Italy, with the contribution of European and international partners, with 60 M€ earmarked in FP9 by EUROfusion, which

reserves the right to propose the first divertor to be tested in DTT. In the present planning, the decision on the first divertor should be taken at end 2022, the construction should be completed in 2025, and the commissioning should be completed at end 2025. The operations should last more than 25 years, starting in 2025 with the first plasma. In the first phases the additional power should be increased up to full performance with single null (SN) configurations. The succeeding phases should be devoted to alternative magnetic configurations, liquid metal divertors, and further upgrades.

B. Physical and technical specifications

DTT is a facility addressed to develop and test integrated power exhaust solutions for DEMO including plasma facing components, control diagnostics and actuators.
The design of DTT is based on the following physical requirements:

- preservation of 4 DEMO relevant parameters: T_e, $\nu^*=L_d/\lambda_{ei}$, Δ_d/λ_0, β, where T_e is the electron temperature, L_d is the divertor field line length, λ_{ei} is the electron-ion collisional mean free path, Δ_d is the SOL thickness, λ_0 is the neutrals mean free path, β is the plasma pressure normalized to the total magnetic pressure;
- slight relaxation on the normalized Larmor radius: $\rho^*=(\rho_i/\Delta_d)$, where ρ_i is the ion Larmor radius;
- integrated scenarios: solutions compatible with plasma performance of DEMO.

In addition, the DTT design take also into account the following technological constraints:

- $P_{sep}/R \geq 15$ MW/m, where P_{sep} is the power crossing the separatrix;
- flexibility in the divertor region to possibly test several divertor concepts;
- possibility to test alternative magnetic configurations;
- possibility to test liquid metals;
- integrated scenarios: solutions compatible with technological constraints of DEMO;
- budget constraint: within 500 M€.

C. Main parameters

The optimization of the DTT design, constrained by the above discussed requirements, led to the definition of a tokamak device with a plasma major radius of 2.11 m in a single null configuration and an additional power coupled to the plasma of 45 MW in the full performance phases. However, in the first years of exploitation, DTT will operate with a reduced additional power mix of about 25 MW: 3 MW from ICRH, 15 MW from ECRH and 7 MW from NBI (Fig. 8).
Figure 9 shows a poloidal cross section of DTT, whereas the main relevant parameters are reported in Table I.

IV. The DTT electromagnetic heart

As is typical for Tokamaks, the electromagnetic aspects of the DTT project are numerous and important and, therefore, attract the interest of many research groups operating in the field of numerical electromagnetism. The correct implementation of the project requires accurate modeling and sophisticated methodologies.
Here, many interesting subsystems of the DTT project could be discussed, such as electromagnetic diagnostics, on- and off-line identification procedures, real time control systems, transport phenomena in the plasma core and SOL, design of the magnet system (Fig. 10), power supplies, heating systems with radiofrequency antennas and neutral beam injections.
For reasons of compactness, only three specific problems will be treated here, all of great interest to the electromagnetic community: coupling between plasma and surrounding conductors (i.e., a typical coupled problem), the computation of electromechanical stresses in complex geometries (i.e., a typical large scale electromagnetic calculation problem) and, finally, the design of the plasma scenario (i.e., a typical optimization problem in electromagnetism). Considering the obvious elements of overlap, the first two applications in DTT will be treated together.

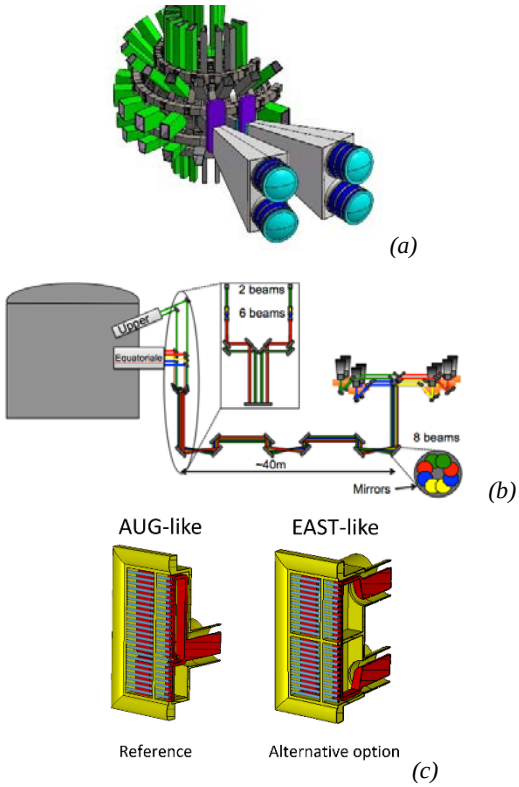

Fig. 8. Systems for heating: a) NBI system; b) ECRH transmission lines; c) ICRH concepts considered for DTT.

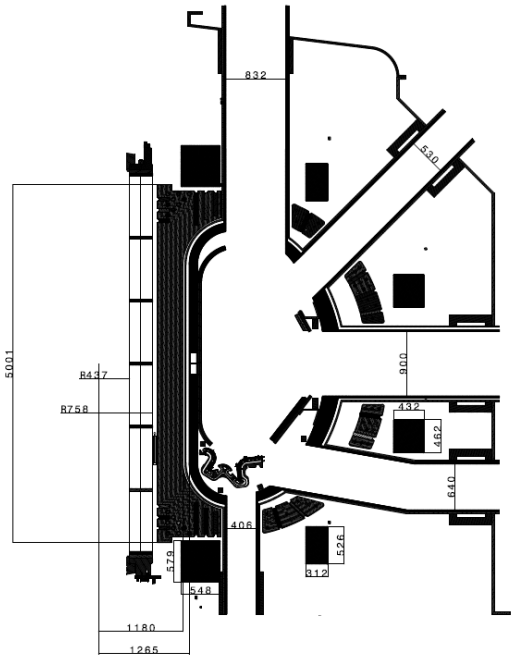

Fig. 9. DTT poloidal cross section (symmetry plane of vessel ports) with all dimensions in mm

TABLE I. MAIN PARAMETERS OF DTT AND ITER

Parameter	DTT	ITER
Major radius R (m)	2.11	6.2
Minor radius a (m)	0.64	2.0
Plasma current Ip (MA)	5.5	15
Toroidal field B_T (T)	6.0	5.3
Plasma volume V_p (m^3)	28	853
Density <n> ($10^{20}m^{-3}$)	1.8	1.0
Greenwald fraction <n>/n_G	0.42	0.85
Additional power P_{tot} (MW)	45	120
Confinement time τ_E (s)	0.43	3.6
Temperature <T> (keV)	6.1	8.5
Total beta β (%)	2.2	2.2
Normalized collisionality ν* (10^{-2})	2.6	2.3
Normalized Larmor radius ρ* (10^{-3})	2.9	2.0
P_{sep}/R (MW/m)	15	14
Power e-folding length λ_q (mm)	1.8	2.2
Pulse length (s)	90	400

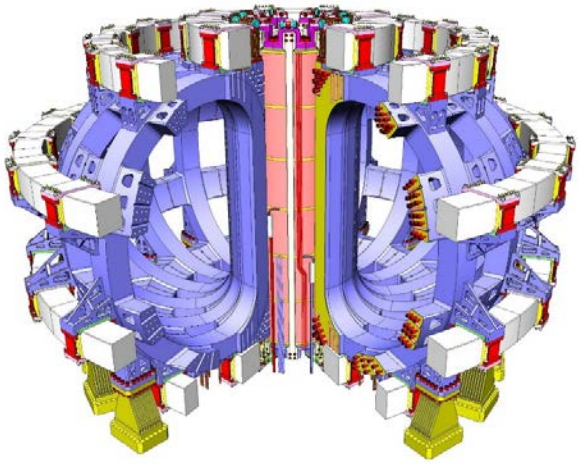

Fig. 10. The DTT superconducting magnet system, with 18 D-shaped TF coils, 6 PF coils, and a central stack of 6 CS modules.

V. ELECTROMAGNETIC COUPLING BETWEEN PLASMA AND SURROUNDING CONDUCTORS

The electromagnetic interaction of the plasma with the surrounding conducting structures rules the dimensioning of many crucial components of a fusion device. Indeed, plasma movements and current changes are affected by external conductors and, in turn, may induce significant eddy currents in the surrounding conductors. From the mathematical point of view, this results in a coupled problem involving electromagnetic equations (describing the external conductors) and the Magneto-Hydro-Dynamic equations (describing the plasma evolution).

The formulation of the CarMa0NL code [10] decouples the electromagnetic interaction between the plasma and the conductors via a suitable surface *S*. Assuming that plasma mass can be neglected, the problem can be formulated as:

$$\begin{array}{l} \textit{Plasma equilibrium equations inside } S \\ \textit{Eddy currents equations outside } S \\ \textit{Coupling conditions on } S \end{array} \qquad (1)$$

In the plasma region, a cylindrical frame of reference (r,z,φ) is introduced and "*pol*" is used to denote the poloidal quantities (i.e. in the r,z plane). The plasma is assumed to be axisymmetric, i.e. no variation along φ takes place. Here Ω denotes the region accessible to the plasma. Its boundary ∂Ω corresponds to the intersection of the coupling surface *S* with the poloidal plane (Fig. 11).

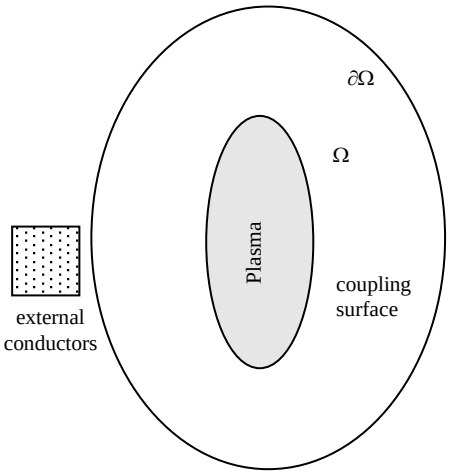

Fig. 11. Reference geometry for the coupled problems in the poloidal plane.

The plasma equilibrium equations in Ω can be written as [10]:

$$\begin{aligned} \nabla_{pol}\cdot\left(\frac{1}{r}\nabla\psi\right) &= j_\varphi(\psi) \ \text{ in } \Omega \\ \psi|_{\partial\Omega} &= \hat{\psi} \end{aligned} \qquad (2)$$

where $\psi(r,z)$ is the poloidal magnetic flux per radian and the nonlinear function $j_\varphi(\psi)$ is the toroidal current density in the plasma. The unknown boundary value $\hat{\psi}$ can be written as:

$$\hat{\psi} = \hat{\psi}_p + \hat{\psi}_e \qquad (3)$$

where "*p*" (resp. "*e*") indicates the contribution to magnetic flux of the plasma currents inside Ω (resp. external currents outside Ω). The quantity $\hat{\psi}_p$ depends obviously on the plasma current density $j_\phi(\psi)$, so it is a nonlinear function of ψ.

Then (2) is written in weak form and discretized it with as second order triangular mesh, leading to a set of nonlinear equation [10]:

$$\underline{F}\left(\underline{\psi},\underline{\hat{\psi}}_e\right) = 0 \qquad (4)$$

where the numerical vectors $\underline{\psi},\underline{\hat{\psi}}_e$ are the values at the nodes of the triangular mesh of the various quantities.

In the conductors, eddy currents equations are solved, by means of an integral formulation, as explained in more details in the following section. This gives rise to a set of discrete number of DoF, $\underline{I}$, describing currents flowing in the conductors.

The magnetic coupling from the structures to the plasma is treated by computing the external poloidal flux on the coupling surface via Biot-Savart integral, which is discretized via a suitable matrix $\underline{Q}$:

$$\underline{\hat{\psi}}_e = \underline{\underline{Q}}\,\underline{I} \tag{5}$$

The magnetic coupling from the plasma to the structure is managed by computing an equivalent (axisymmetric) surface current density, located on the coupling surface *S*, producing the same magnetic field as the plasma outside *S*. From the computational point of view, this surface current density is computed by fictitiously imposing that *S* is the surface of a perfect conductor, able to completely shield the field outside *S*, using a filamentary discretization.

VI. The Eddy Current Integral Formulation

The list of conducting structures of the DTT tokamak includes the vacuum vessel, the divertor plates, the casings of the superconducting coils. Differently from the reactor layout the complex blanket modules are not present in DTT; therefore, remaining conducting parts are mainly characterized by thin structures, in which the eddy current density is mainly uniformly distributed along their thickness, during the fast transients characterizing both the normal operation (e.g. plasma start-up, shape and position control, shut-down) and possible accidental conditions (e.g. plasma disruptions, failure of a superconducting coil).

From the electromagnetic point of view, the main effects produced during normal operations are the delay in the penetration of the electromagnetic fields inside the vacuum vessel, losses in the superconductors, influence of the control of plasma position and shape. The accurate electromagnetic description of the passive structures and of their coupling with both the plasma during its evolution, and with the active external coils, is of paramount importance. The interest is driven by the need of a deeper comprehension of the physical behavior of the DTT device, in view of its design, but also of the design and operation of future reactors. More specifically, this modeling task is fundamental for several aspects, including the assessment of the main time constants of the conducting structures, the evaluation of the electromagnetic loads, the analysis and verification of its components, the design and characterization of the control system, the simulation of the experiment in its global aspects.

Volume integral formulations appear to be particularly attractive for this electromagnetic analysis for several reasons. The main advantages are: (i) the spatial domain external to the conductors does not need to be discretized and (ii) the regularity conditions at infinity are naturally satisfied. Moreover, in the boundary integral formulations where the unknowns are only localized on conductors surface, additional complexities arise when treating, as often required in the present analysis, piecewise homogeneous objects, characterized by small thickness.

The approach is able to effectively treat thin structures, including complex anisotropic conducting media and a natural coupling with voltage and current sources.

The numerical model is here shortly described [11, 12]. Expressing the magnetic vector potential **A**, uniquely defined by the Coulomb gauge, by means of the Biot Savart integral in terms of the current density sources, we obtain the following integral equation:

$$\begin{aligned} &\eta\mathbf{J}(\mathbf{x},t) + \frac{\mu_0}{4\pi}\frac{\partial}{\partial t}\int_{V_c}\frac{\mathbf{J}(\mathbf{x}',t)}{|\mathbf{x}-\mathbf{x}'|}d\tau' + \nabla\varphi(\mathbf{x},t) = -\frac{\partial\mathbf{A}_0}{\partial t} \\ &\mathbf{J}(\cdot,t)\in S \square \left\{\mathbf{v}\in\mathbf{H}(div,V_c), \nabla\cdot\mathbf{v}=0 \text{ in } V_c, \mathbf{v}\cdot\hat{\mathbf{n}}=0 \text{ in } \partial V_c\right\} \\ &\mathbf{J}(\mathbf{x},0) = \mathbf{J}_0(\mathbf{x}) \end{aligned} \tag{6}$$

where η is the electric resistivity tensor, φ is the electric scalar potential, $\mathbf{J}_0$ is the prescribed initial condition and $\mathbf{A}_0$ is the magnetic vector potential due to the sources external to the conducting domain V_c. The divergence free current density induced in the conducting passive structure is expressed as the curl of the electric vector potential. The uniqueness of this potential is assured, at the discrete level, using edge elements shape functions and the tree-cotree gauge. Projecting. (6) on the finite dimensional space of the edge base functions $\mathbf{J}_k(\mathbf{x}) = \nabla\times\mathbf{T}_k$, belonging to the set *S*, the following linear system is obtained:

$$\underline{\underline{L}}\frac{d\underline{I}}{dt} + \underline{\underline{R}}\,\underline{I} = \underline{V} \tag{7}$$

where

$$L_{ij} = \frac{\mu_0}{4\pi}\int_{V_c}\int_{V_c}\frac{\mathbf{J}_i(\mathbf{x})\cdot\mathbf{J}_j(\mathbf{x}')}{|\mathbf{x}-\mathbf{x}'|}d\tau\, d\tau'$$

$$R_{ij} = \int_{V_c}\mathbf{J}_i(\mathbf{x})\cdot\eta\mathbf{J}_j(\mathbf{x})d\tau$$

$$V_i = \int_{V_c}\mathbf{J}_i(\mathbf{x})\cdot\frac{\partial\mathbf{A}_0(\mathbf{x},t)}{\partial t}d\tau$$

Multiply connected domains are automatically taken into as described in [13], where also an efficient way for including the electric circuit equations in the numerical model is illustrated.

This formulation, for the large magneto-quasi-static (MQS) problems arising in the analysis of a tokamak, can be extremely effective in terms computational cost, if suitable strategies are adopted. Indeed, the matrix *L* is fully populated and its building up cost scales as N^2, where *N* is the number of degrees of freedom, whereas the computational cost to solve the system through a direct method scales as N^3. In order to reduce these costs, suitable sparsification techniques have been proposed such as, Fast Fourier Transform [14], Fast Multipole Method [15] or SVD [16], taking advantages of the low rank property of the submatrices describing the far interactions, along with parallel computation techniques.

VII. Plasma Scenario Design and Optimization

A plasma scenario is defined as the sequence of plasma configurations characterizing the most important phases of a plasma discharge, as shown in Fig. 12. After the plasma breakdown, obtained by a null hexapolar point of the magnetic flux surfaces in the center of plasma chamber with a proper electric field, a low current plasma takes place. In this phase, the plasma configuration is called *limited* and it characterized by a contact point between the last plasma surface and first wall. To avoid damages to the first wall during plasma current ramp up, a transition from a *limited* configuration to a *diverted* plasma is imposed. In a divertor configuration, a null point of the magnetic field is imposed inside the chamber allowing a last plasma surface to be sustained on an X-point without a first wall contact point.

Once the plasma ramp-up is concluded, the scenario reaches the flat-top phase where the hot plasma is sustained by the active

coils as long as possible and the best fusion performance can be achieved. During the flat top phase, the ohmic losses are balanced by external additional heating and by the current induced by the central solenoid acting as the primary winding of a transformer. The plasma scenario is concluded after the plasma current ramp-down that allows a safe shut down.

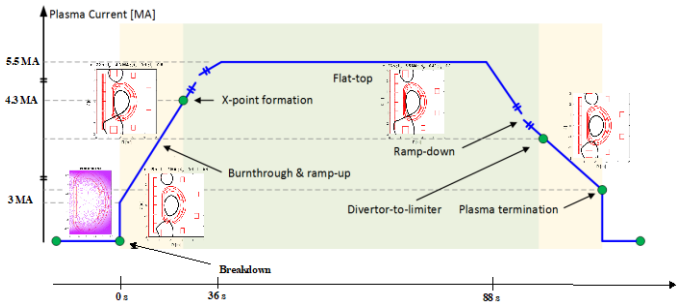

Fig. 12. Reference plasma scenario in DTT.

The electromagnetic modelling assumes a key role for the definition and optimization of the plasma scenario in a tokamak. Its importance is even emphasized in the DTT device whose aim is to consider possible alternative plasma configurations in order to tackle the power exhaust problem.

In the following, the electromagnetic modeling of the plasma equilibrium will be presented in the axisymmetric case. Moreover, the optimization problem of a single scenario snapshot will be formalized with an application to the DTT device case.

A. Plasma Modelling

For the scenario optimization, the system schematized by the plasma, the passive structures and the active circuits. The 2D FEM code CREATE-NL [17] is designed to solve numerically the Grad-Shafranov equation, which describes the behavior of such a system under the hypothesis of axial symmetry. The output of the code is a static plasma equilibrium.

Both CREATE-NL and CREATE-L [17-18] can be used to obtain a linearized model by means of two different linearization procedures, numerical and analytical in a neighborhood of the equilibrium point, respectively. The general form of a linearized model can be derived from the following set of variables:

- $\delta\underline{x}(t) = \left[\delta\underline{I}_{CS/PF}(t)\ \delta\underline{I}_{e}(t)\ \delta\underline{I}_{p}(t)\right]^{T}$ is the current vector which includes external currents and plasma current;
- $\delta\underline{u}(t)(t) = \left[\delta\underline{U}_{CS/PF}(t)\ \right]^{T}$ is the input vector composed by voltages on the poloidal field coils;
- $\delta\underline{w}(t) = \left[\delta\beta_{pol}(t)\ \delta l_i(t)\right]^{T}$ is the disturbance vector where β_{pol} and l_i are parameters related to the plasma internal distributions of pressure and toroidal current density, respectively. This choice is made according to the assumptions and the analyses described in [19];
- $\delta\underline{y}(t) = \left[\delta\underline{\psi}(t)\ \delta\underline{B}_{pol}\ \delta\psi_b(t)\ \delta\underline{g}(t)\right]^{T}$ is the output vector including: poloidal magnetic fluxes per radian $\delta\psi(t)$ and poloidal magnetic fields δB_{pol} measured by the diagnostic system, $\delta\psi_b(t)$, the magnetic flux per radian at the plasma boundary, and $\delta g(t)$, the plasma wall gaps at different poloidal locations of the first wall/divertor.

Linearization around equilibrium quantities $\underline{X}_0, \underline{W}_0$ and $\underline{Y}_0$ yields:

$$\begin{aligned}\delta\dot{\underline{x}}(t) &= \underline{\underline{A}}\delta\underline{x}(t) + \underline{\underline{B}}\delta\underline{u}(t) + \underline{\underline{E}}\delta\underline{w}(t)\\ \delta\underline{y}(t) &= \underline{\underline{C}}\delta\underline{x}(t) + \underline{\underline{F}}\delta\underline{w}(t)\end{aligned} \tag{8}$$

where:

- $\delta\underline{x}(t) = \underline{X}(t) - \underline{X}_0$;
- $\delta\underline{w}(t) = \underline{W}(t) - \underline{W}_0$;
- $\delta\underline{y}(t) = \underline{Y}(t) - \underline{Y}_0$;
- $\underline{\underline{A}} = -\underline{\underline{L}}^{-1}\underline{\underline{R}}$ is the dynamical matrix with R and L the resistance and inductance matrices, respectively;
- $\underline{\underline{B}} = \underline{\underline{L}}^{-1}$ is the input matrix;
- $\underline{\underline{E}} = -\underline{\underline{L}}^{-1}\underline{\underline{L}}_E$ is the disturbance matrix with $\underline{\underline{L}}_E$ used to take into account possible plasma profile variations on the state variables;
- $\underline{\underline{C}}$, $\underline{\underline{F}}$ are output model matrices: $\underline{\underline{C}} = \left(\partial\underline{Y}/\partial\underline{X}\right)_W$, $F = \left(\partial\underline{Y}/\partial\underline{W}\right)_X$.

Among the outputs of the linearized model y(t), particular importance is assumed by the so-called *gaps* $\underline{g}$, the measurements of the plasma–wall distances in different parts of the plasma region. Resorting to the linearized equations (8), small variations of the currents in the CS/PF coils ($\delta\underline{I}_{CS/PF}$) are related to small variations of the plasma shape ($\delta\underline{g}$) through a coefficient matrix ($\underline{\underline{C}}_G$):

$$\delta\underline{g} = \underline{\underline{C}}_G\delta\underline{I}_{CS/PF}. \tag{9}$$

Although the relation between the variation of the gaps and the PF currents is not linear, if the plasma boundary does not change too much, a linearization in (8)-(9) represents an important tool for the optimization of the PF coil system for a given set of plasma configurations.

B. Plasma snapshot optimization

The definition of a plasma scenario requires to consider different sets of constraints posed by the mechanical structures (maximum stress on the conductive structure), by the actuator limits (maximum currents and voltages on the active coils) and by the plasma scenario operational constraints (e.g., bounds on the possible variations of the plasma parameters).

The scenario design procedure is based on the solution of an optimization problem implemented on the linearized model of the plasma, as stated in equation (8). In this section the design and optimization of a single plasma scenario snapshot is focused. The procedure is implemented in terms of a quadratic optimization problem with linear and quadratic constraints. The idea beneath the optimization procedure is the definition of a linearized model that relates the variation of the currents in the redundant CS/PF coil system $\delta I_{CS/PF}$ to the variation of the quantities related to the constraints listed above.

The optimization problem, neglecting the force constraints, can be stated as follows:

$$\min_{\delta\underline{I}_{\mathrm{CS/PF}}} \left(\underline{I}_{eq} + \delta\underline{I}_{\mathrm{CS/PF}}\right)^{T}\underline{\underline{W}}\left(\underline{I}_{eq} + \delta\underline{I}_{\mathrm{CS/PF}}\right) \tag{10}$$

subject to

$$\left\|\Delta \underline{G}_{des} - \underline{\underline{C}}_{G}\delta \underline{I}_{\mathrm{CS/PF}}\right\| < \Delta \underline{g} \quad (11.1)$$

$$\left\|\underline{B}_{eq} + \underline{\underline{C}}_{B_{pol}}\delta \underline{I}_{\mathrm{CS/PF}}\right\| < B_{max} \quad (11.2)$$

$$\left\|\underline{I}_{eq} + \delta \underline{I}_{\mathrm{CS/PF}}\right\| < I_{max} \quad (11.3)$$

$$\left\|\Delta \psi_{b,des} - \underline{\underline{C}}_{\psi_b(t)}\delta \underline{I}_{\mathrm{CS/PF}}\right\| < \epsilon \quad (11.4)$$

where

- $\underline{I}_{eq} \in R^n$ is the vector of the CS/PF currents of the equilibrium used for the generation of the linearized plasma model;
- $\underline{B}_{eq} \in R^n$ is the vector of the poloidal magnetic field in the coil locations of the equilibrium used for the generation of the linearized plasma model;
- $\delta \underline{I}_{\mathrm{CS/PF}}$ are the optimized CS/PF current variations in the active coils. The total optimized currents are $\underline{I}_{opt} = \underline{I}_{eq} + \delta \underline{I}_{\mathrm{CS/PF}}$;
- $\Delta \underline{G}_{des}$ indicates the desired gaps variations with respect to the equilibrium used for the generation of the linearized plasma model;
- $\Delta \underline{g}$ indicates the tolerance for the tracking of $\Delta \underline{G}_{des}$;
- $\Delta \psi_{b,des}$ indicates the desired boundary flux variation with respect to the equilibrium used for the generation of the linearized plasma model;
- $\underline{\underline{C}}_{\Psi_b(t)}$ is the output matrix related to the magnetic flux at the plasma boundary and ϵ indicate the tolerance for the tracking of $\Delta \psi_{b,des}$ (ideally $\epsilon \to 0$);
- $\underline{\underline{W}}$ is a weighting matrix.

The inequalities (11) can be easily converted into linear constraints with respect to the optimization variables, defining, together with the quadratic objective function (10), a convex LQ optimization problem [20-21].

The vertical force constraints on the active coils are proportional to the currents flowing in the coils and to the radial magnetic field in the coil locations. Hence, for an almost fixed plasma shape and current, a quadratic dependence of the vertical forces on the PF/CS currents can be imposed [22]. It gives rise to the definition of a non-convex optimization problem whose solution is strongly affected by the initial condition.
The maximum voltage constraint is inherent of the overall scenario optimization and it can be performed once the single snapshots are produced and associated to a fixed time instant.

VIII. Examples of Application to DTT

A. Plasma disruption in DTT

Here an application of the procedure is shown for a possible plasma disruption event in DTT.
Figure 13 reports the triangular mesh used in the plasma region and the coupling surface used for the computation. The main vessel is a double-walled torus with "D" shaped cross-section, segmented in 14 standard modules (20°) whose access ports are designed to satisfy requirements coming from diagnostic system, heating system, pumping system and Remote Handling system and a Negative Neutral Beam Injectors module (80°) able to host two adjacent neutral beam injectors at the equatorial level. The thickness of both the inner and the outer shells, AISI 316L(N) stainless steel, is assumed equal to 15 mm. In Fig. 14, the discretization of the vacuum vessel in the external region is shown.

The evolution of the plasma has been analyzed during a disruptive event, defined by a fast loss of plasma thermal energy, followed by a decay of the plasma current, starting from the reference equilibrium. Figure 15 shows some snapshots of the plasma evolution, while Fig. 16 reports a sample pattern of the eddy current induced in the vessel.

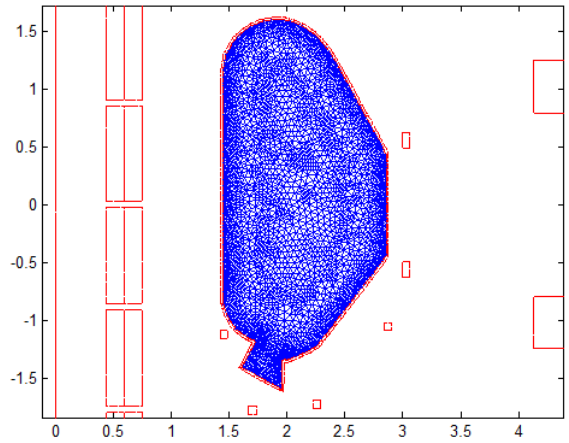

Fig. 13. Triangular mesh in the plasma region and coupling surface. The cross section of some axisymmetric external conductors is also reported.

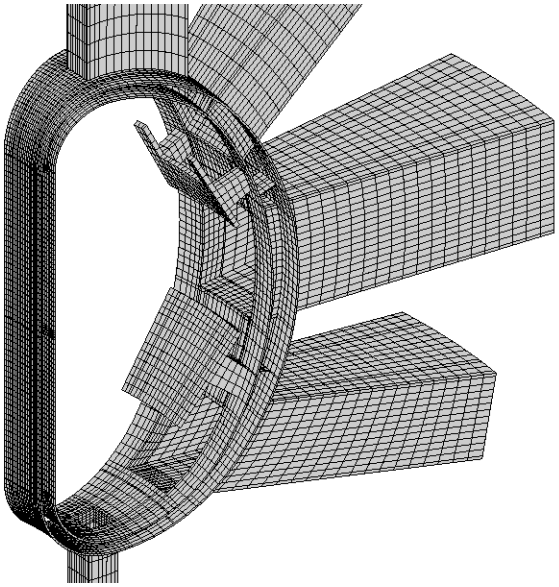

Fig. 14. Finite elements mesh of the vessel (divertor is not reported).

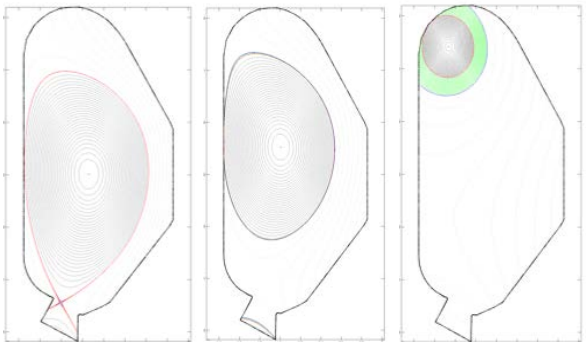

Fig. 15. Sample snapshots of the plasma configuration during the disruption.

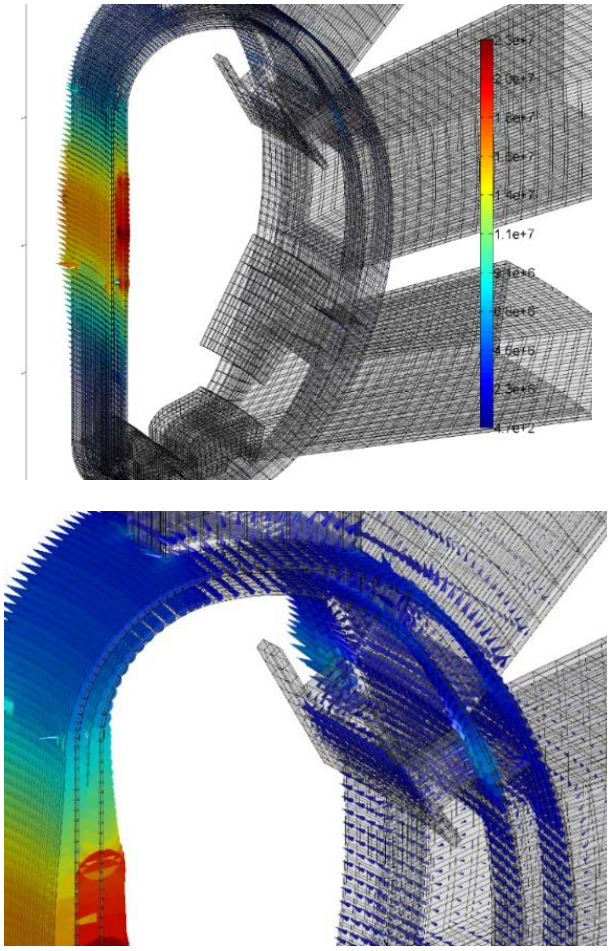

Fig. 16. Two details of a typical eddy current distribution induced in the vacuum vessel of DTT by a plasma disruption.

B. Scenario optimization in DTT

The optimization procedure (10)-(11) has been used for the premagnetization (Fig. 17) as well as for the definition of all the DTT plasma configurations, as illustrated in Fig. 18, where additional specific constraints have been considered for each alternative plasma configurations.

IX. Next 25 years: A challenging perspective

The DTT program, with its important investment of financial and human resources, offers a significant opportunity for technology transfer and experimentation of advanced technologies, at service of the international production world.

The project is also a stimulating gym for the international scientific community and, in particular, for that of numerical electromagnetism, in which to assess mathematical models and numerical procedures in a demanding and innovative application.

The realization of the DTT will also be an important job opportunity for highly qualified engineers, physicists and technicians from all countries.

Finally, the DTT will also be a challenging opportunity for young researchers and PhD School students to have, "on the job", high standard experiences in a stimulating and qualified international scientific environment.

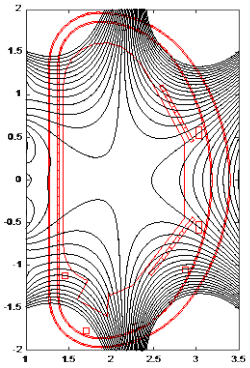

Fig. 17. Premagnetization of DTT: poloidal flux map. The flux linked with the plasma is 16.2 Vs with a region of about 0.7 m^2 where the poloidal field is less than 5 mT, whereas the toroidal field is 6.0 T.

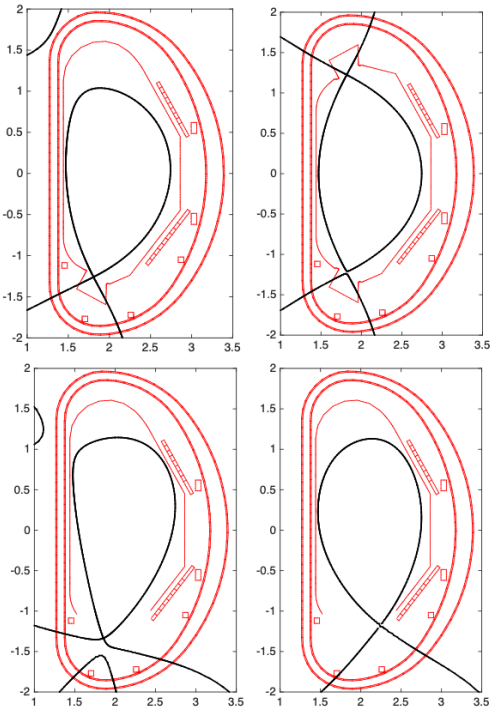

Fig. 18. DTT flat top configurations: single null (top-left), double null (top-right), snowflake (bottom-left) and negative triangularity (bottom-right)

X. References

[1] Chen, F., *Introduction to Plasma Physics and Controlled Fusion*, Plenum Press, 2010.

[2] http://www.iter.org/.

[3] Spitzer, L., “The Stellarator Concept”, Physics of Fluids, 1958, 253-264.

[4] Bodin, H.A., Newton, A., “RFP Research”, *Nuclear Fusion*, 1980, 1255-1324.

[5] Wesson, J., *Tokamaks*, Oxford University Press, 2005.

[6] European Research Roadmap to the Realization of Fusion Energy, November 2018 (https://www.euro-fusion.org/fileadmin/user_upload/EUROfusion/Documents/2018_Research_roadmap_long_version_01.pdf).

[7] Loarte, A., Neu, R., “Power exhaust in tokamaks and scenario integration issues”, *Fusion Engineering and Design*, 2017, 256-273.

[8] Albanese, R., et al. Eds., “DTT Divertor Tokamak Test facility”, *Special Section of Fusion Engineering and Design*, 2017, 253-294 and e1-e25.

[9] Martone, R., et al. Eds., “DTT Divertor Tokamak Test facility – Interim Design Report”, ENEA, ISBN: 978-88-8286-378-4, 2019 (https://www.dtt-project.enea.it/downloads/DTT_IDR_2019_WEB.pdf).
[10] Villone, F., et al., "Coupling of nonlinear axisymmetric plasma evolution with three-dimensional volumetric conductors", *Plasma Physics and. Controlled Fusion*, 2013.
[11] Albanese, R., Rubinacci, G., "Integral formulation for 3D eddy-current computation using edge elements", *IEEE Proceedings — A*, 1988, 457-462.
[12] Albanese, R., Rubinacci, G., “Finite Element Methods for the Solution of 3D Eddy Current Problems”, *Advances in Imaging and Electron Physics*, P. W. Hawkes Ed., 1998, Academic Press, 1998, 1-86.
[13] Rubinacci, G., Tamburrino, A., Villone, F., “Circuits/Fields Coupling and Multiply Connected Domains in Integral Formulations”, *IEEE Transactions on Magnetics*, 2002, 581-584.
[14] Rubinacci, G., Tamburrino, A., Ventre, S., Villone, F., “A Fast Algorithm for Solving 3D Eddy Current Problems with Integral Formulations”, *IEEE Transactions on Magnetics*, 2001, 3099-3103.
[15] Rubinacci, G., Tamburrino, A., Ventre, S., Villone, F., “A fast 3-D multipole method for eddy-current computation”, *IEEE Transactions on Magnetics*, 2004, 1290-1293.
[16] Rubinacci, G., Ventre, S., Villone, F., Liu, Y., “A fast technique applied to the analysis of Resistive Wall Modes with 3D conducting structures”, *Journal of Computational Physics*, 2009, 1562–1572.
[17] Albanese, R., Ambrosino, R., Mattei, M., “CREATE-NL+: A robust control-oriented free boundary dynamic plasma equilibrium solver”. *Fusion Engineering and Design*, 2015, 664-667.
[18] Albanese, R., Villone, F., “The linearized CREATE-L plasma response model for the control of current, position and shape in tokamaks”, *Nuclear Fusion*, 1998, 723-738.
[19] Luxon, J.L., Brown, B.B., “Magnetic analysis of non-circular cross-section tokamaks”, *Nuclear Fusion*, 1982, 813.
[20] Potra, F. A., Wright, S.J., “Interior-point methods”, *Journal of Computational and Applied Mathematics*, 2000, 281-302.
[21] Coleman, T. F., Li, Y., “A Reflective Newton Method for Minimizing a Quadratic Function Subject to Bounds on Some of the Variables”, *SIAM Journal on Optimization*, 1995, 1040-1058.
[22] Albanese, R., Ambrosino, R., Castaldo, A., Lo Schiavo, V.P., “Optimization of the PF coil system in axisymmetric fusion devices”, *Fusion Engineering and Design*, 2018, 163-172.

ACKNOWLEDGMENTS

The authors would like to thank all the contributors of “DTT Divertor Tokamak Test facility – Interim Design Report” [9] for the useful discussion.

AUTHORS NAME AND AFFILIATION

R. Martone[(1,2)], R. Albanese[(2,3)], R. Ambrosino[(2,3)], T. Bolzonella[(4)], A. Castaldo[(2)], R. Fresa[(2,5)], V.P. Loschiavo[(2)], G. Ramogida[(6)], G. Rubinacci[(2,3)], F. Villone[(2,3)], S. Ventre[(2,7)]

[(1)] Università degli Studi della Campania, Italy
[(2)] Consorzio CREATE, Napoli, Italy
[(3)] Università degli Studi di Napoli Federico II, Italy
[(4)] Consorzio RFX, Padova, Italy
[(5)] Università degli Studi della Basilicata, Potenza, Italy
[(6)] Enea, CR Frascati (Roma), Italy
[(7)] Università degli Studi di Cassino e del Basso Lazio, Italy

Corresponding author: raffaele.martone@unicampania.it

https://www.compumag.org/wp/